Research article

Wei-Chun Wang, Huai-Yung Wang, Tzu-Yu Chen, Cheng-Ting Tsai, Chih-Hsien Cheng, Hao-Chung Kuo and Gong-Ru Lin*

CdSe/ZnS core-shell quantum dot assisted color conversion of violet laser diode for white lighting communication

https://doi.org/10.1515/nanoph-2019-0205
Received July 2, 2019; revised August 13, 2019; accepted September 20, 2019

Abstract: By color-converting the violet laser diode (VLD) with a cadmium selenide and zinc sulfide (CdSe/ZnS) core-shell-quantum dot (QD) doped polydimethylsiloxane (PDMS) film, the VLD + CdSe/ZnS core-shell-QD transferred white-light with improved color rendering index (CRI) is demonstrated for high-speed indoor visible lighting communication. To facilitate hue saturation value (HSV) of the VLD + CdSe/ZnS core-shell-QD white-lighting module, dual-sized CdSe/ZnS core-shell-QDs with two luminescent wavelengths centered at 515 and 630 nm are doped into the PDMS. The CdSe/ZnS core-shell-QD doped PDMS phosphor with the optimized thickness of 2.5 mm serves as the beam divergent color-converter, which not only excites red (R) and green (G) fluorescence to detune the correlated color temperature (CCT) and CRI of the mixed red/green/violet (RGV) white-light, but also remains the residual VLD signal for data transmission. With a divergent angle of 127°, such a VLD + CdSe/ZnS core-shell-QD can deliver cold white-light with a CCT of 6389 K and a CRI of 63.3 at Commission International de l'Eclairage coordinate of 0.3214, 0.2755. Most important, the residual VLD light component is relatively weak with its wavelength out of the peak optical sensitivity region of the human retina centered at 441 nm. The directly encoded VLD + CdSe/ZnS core-shell-QD white light successfully carries the 16-quadrature amplitude modulation (QAM) discrete multitone data, which supports the maximal transmission data rate of 9.6 Gbit/s with a bit error ratio (BER) of 3.59×10^{-3}.

Keywords: visible light communication; white-lighting; CdSe/ZnS core-shell quantum dot.

1 Introduction

Recently, visible light communication (VLC) has been considered as a promising communication system for various applications such as indoor white-lighting optical wireless communication (OWC), long-distance underwater wireless optical communication (UWOC), and vehicle-to-vehicle sensing and communications. In contrast to the traditional fiber-optic communication system, the light-fidelity (Li-Fi) is able to provide comparable data transmission rates with better spatial flexibility in the unregulated band, which allows it to serve as the supplement of the existent Wi-Fi access network so as to relieve the congested data traffic. Moreover, the optical wave with electromagnetic immunity can avoid the interference with electronic signals to facilitate its applicability in hospitals, space shuttles and airplane cabins where Wi-Fi is not always available. Furthermore, by integrating the transmitter with the existing lighting equipment, or by directly color-converting its output for lighting, such a white-lighting OWC access network can offer both indoor-lighting and high-speed communication. Taking this advantage, many white-lighting OWC systems based on light-emitting diode (LED) transmitter have been reported previously.

Typically, there are two ordinary schemes to design a white-light LED, including either covering a blue LED with

***Corresponding author: Gong-Ru Lin,** Graduate Institute of Photonics and Optoelectronics, Department of Electrical Engineering, National Taiwan University, No. 1, Roosevelt Rd, Sec. 4, Taipei 10617, Taiwan, R.O.C., e-mail: grlin@ntu.edu.tw. https://orcid.org/0000-0003-2061-1282
Wei-Chun Wang, Huai-Yung Wang, Cheng-Ting Tsai and Chih-Hsien Cheng: Graduate Institute of Photonics and Optoelectronics, Department of Electrical Engineering, National Taiwan University, Taipei 10617, Taiwan, R.O.C.
Tzu-Yu Chen and Hao-Chung Kuo: Graduate Institute of Electro-Optical Engineering, Department of Photonics, National Chiao Tung University, Hsinchu 30100, Taiwan, R.O.C.

phosphor material or combining red/green/blue (RGB) LEDs together for color conversion. In 2008, a VLC system using multiple-resonant equalization with 16 white-light LEDs was proposed for carrying nonreturn-to-zero on-off keying (NRZ-OOK) data at a bit rate of 40 Mbit/s [1]. Later on, Vucic et al. used an off-the-shelf phosphorescent white-light LED to construct a white-lighting OWC system for transmitting discrete multitone (DMT) data at 513 Mbit/s [2]. In 2012, Khalid et al. reported a 1-Gbit/s OWC system based on a phosphorescent white-light LED with the rate-adaptive DMT modulation scheme [3]. In the same year, the RGB LEDs-based Li-Fi system with single-channel and wavelength-division-multiplexing (WDM) link was presented by Cossu et al. for transmitting DMT signal at data rates of 1.5 and 3.4 Gbit/s [4]. Remarkably, Wu et al. further compared the transmission performance of the quadrature amplitude modulation-orthogonal frequency division multiplexing (QAM-OFDM) and the carrier-less amplitude and phase (CAP) modulated data, which were carried by a single set of RGB LEDs to approach transmission capacities of 2.93 and 3.22 Gbit/s in 2013 [5]. To take a step forward for the bi-directional WDM VLC, both RGB LEDs and phosphor-based LED were employed for 575-Mbit/s downstream and 225-Mbit/s upstream transmissions by Wang et al. [6]. To further expand the modulation bandwidth of the white-lighting Li-Fi systems, various equalization techniques and modulation schemes have been employed to restrain the inter-symbol interference (ISI) caused by LEDs. In 2015, Wang et al. employed a single commercial RGB LED module under the CAP modulation with a recursive least square algorithm based adaptive equalization for transmitting through a 1.5-m free-space link at a data rate as high as 4.5 Gbit/s [7]. Afterwards, Huang et al. used a commercial white-light LED to transmit the QAM-OFDM data at 2 Gbit/s over a 1.5-m free-space link [8]. In 2018, Philips demonstrated the LiFi-enabled LED light bulb practically in its smart office at a bit rate of 30 Mbit/s [9]. On the other hand, the micro-LED (μ-LED) has been considered as an advanced candidate for the LED-based OWC system to enlarge the maximal data transmission rate owing to its reduced capacitance at high current density. In 2016, Bamiedakis et al. utilized a gallium nitride (GaN) μ-LED, that directly modulated with the pulse amplitude modulation (PAM) data stream, to set up a 2-Gbit/s OWC link over 0.6 m [10]. In the meantime, Ferreira et al. compared the transmission performance of OOK, PAM, and OFDM data formats carried by a GaN based μ-LED with its operational bandwidth of larger than 800 MHz for achieving the data rate of 1.4, 3.4, and 5 Gbit/s, respectively [11]. Subsequently, a violet μ-LED carried DMT data with a transmission rate of higher than 10 Gbit/s was demonstrated by Islim et al. in 2017 [12]. Although μ-LEDs could provide broader modulation bandwidth than conventional LEDs, their transmission performance is still limited by the significant efficiency droop under high current injection.

More recently, the GaN laser diode (LD) with higher brightness, higher efficiency, higher coherence and broader modulation bandwidth than LED has emerged as the new-class transmitter for visible laser light communication (VLLC) with improved transmission capacity. In 2015, Chi et al. reported a premier demonstration of the GaN LD based VLLC for 64-QAM OFDM data transmission over 5 m at 9 Gbit/s [13]. To involve white-lighting function, Lee et al. employed a blue LD covered with yellow phosphor for carrying NRZ-OOK data at 2 Gbit/s [14]. Subsequently, Retamal et al. elevated the data rate to 4 Gbit/s by employing a blue LD with a remote phosphor-film [15]. Progressively, Chi et al. introduced a VLLC with blue LD and cerium-doped yttrium aluminum garnet (YAG:Ce^{3+}) based phosphor diffuser to upgrade the transmission data rate to 5.2 Gbit/s [16]. Chun et al. proposed a dual-LD and remote phosphor white-light VLLC for 5.6/6.5 Gbit/s data transmission [17]. In 2018, Wu et al. used blue LD adhered with a phosphor film to reach 4.4-Gbit/s data transmission [18]. Alternatively, the white-lighting VLLC constructed by RGB LDs with a data rate beyond 8 Gbit/s has been proposed by Tsonev et al. [19] Likewise, Janjua et al. used the fiber-pigtailed RGB LDs to reach a data rate of >4 Gbit/s for each colored channel [20]. Wu et al. also demonstrated similar OWC system at 8.8 Gbit/s with TO-can packaged RGB LDs [21]. Although the RGB-LD mixed white-light scheme can provide higher total data transmission rate, its setup is more complex, and the transmission capacity per channel is much lower than a single phosphorescent white-light LD. Besides, the much narrower linewidth of the LD as compared to the LED usually leads to the lower color rendering index (CRI) of the white-light for indoor lighting. Considering the abovementioned drawbacks, the phosphor color-converted blue/violet LD with higher CRI and data rate becomes the compact and cost-effective solution for white-lighting VLLC. In 2017, Chi et al. preliminarily employed a phosphor converted violet laser diode (VLD) for white-lighting VLLC at 4.4 Gbit/s with a high CRI of 89.1 [22], which experimentally proved that a VLD-based light source can provide high-quality indoor white-lighting communication. Moreover, Lee et al. used a 410-nm VLD pumped RGB phosphor white-light source for data transmission beyond 1 Gbit/s with a CRI of 79 [23].

In addition to the selection among different transmitters, the phosphor material is also a key point as which can affect the transmission performance due to its finite

luminescent lifetime. The long lifetime of the commercial phosphor is always the bottleneck to limit the allowable data rate of the white-lighting LED VLC system. Accordingly, several alternative color converters with shortened photon lifetime have been reported recently. In 2014, Chun et al. reported a white-lighting VLC system composed of a μ-LED and a yellow fluorescent polymer with a radiative lifetime of shorter than 1 ns [24]. Later on, Sajjad et al. proposed organic semiconductors based on BODIPY, BBEHP-PPV, and MEH-PPV with high photoluminescence quantum yields (PLQYs) and very short lifetime for LED based VLC system to reach an improved frequency response and modulation bandwidth [25, 26]. Afterwards, Dursun et al. employed a perovskite nanocrystal with a radiative recombination lifetime of only 7 ns to generate white light with a CRI of 89 in 2016 [27]. Subsequently, Wang et al. reported a dye-loaded metal-organic hybrid framework with a lifetime of few ns for white-light LED [28]. Leitao et al. utilized colloidal semiconductor quantum dots (QDs) with a lifetime of ~10 ns as the fast color converter for μ-LED-based white-lighting VLC [29]. Moreover, Yang et al. reported a nanopatterned hyperbolic metamaterial covered by a fluorescent polymer with fast response to enhance the data bandwidth [30]. Lately, Xiao et al. designed a white-light LED based on cadmium selenide (CdSe)/zinc sulfide (ZnS) QDs with red/green luminescent time as short as 26 ns to improve modulation bandwidth [31]. This declared that the QD-based color converter is a promising candidate for the next generation white-lighting VLC system with exceptional advantages including tunable emission wavelength, adjustable lifetime, fast radiative response, and high quantum yield. Nonetheless, the QD-based color converter has yet to be used for the VLD based VLC up to now. Another important reason to develop the VLD based white-lighting source is to prevent the blue-light hazard to human eyes, as the residual VLD light component in the mixed white-light is relatively weak with its wavelength out of the peak optical sensitivity region of the human retina at 441 nm.

In this work, for the first time, a 405-nm TO-can package VLD color-converted with phosphor QDs was employed as the white-lighting transmitter of the VLLC system. The 16-QAM DMT data stream was employed to deliver in such a 0.5-m free-space VLLC link. The polydimethylsiloxane (PDMS) film doped by dual-sized CdSe/ZnS core-shell QDs with dual luminescent wavelengths is served as the color converter for white-light generation, in which the utilized CdSe/ZnS core-shell-QD particles with two emission bands and different mixing ratios are adjusted in advance to reach the desirable correlated color temperature (CCT) for indoor lighting. Subsequently, the CCT, CRI, illuminance, and divergent angle are, respectively determined to estimate the white-lighting performance of the proposed VLD + CdSe/ZnS core-shell-QD light source. During the analysis of the transmission performance, the bias current of the VLD, the sampling rate of the arbitrary waveform generator (AWG), and the pre-leveled slope of the DMT subcarrier power are precisely optimized to achieve the ultimate modulation bandwidth for 16-QAM DMT data stream.

2 Experimental setup

Firstly, a TO-38-can package VLD at violet-blue wavelength was employed as both the lighting and transmitting source for the white-light VLC, as shown in Figure 1A. In addition, the CdSe/ZnS core-shell QD was used to perform the color conversion, as shown in Figure 1B. In more detail, the TO-38-can package VLD was plugged into a Sub-Miniature version A (SMA) connector and connected to a bias-tee, and then mounted on a self-designed copper-based heat sink. It was fixed to a homemade copper sink

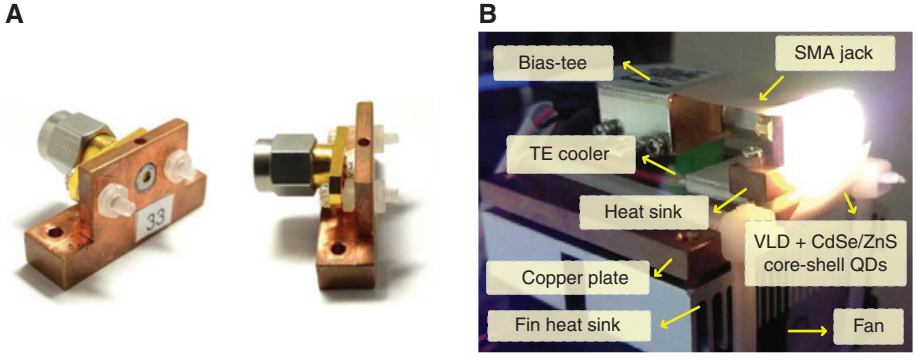

Figure 1: The VLD based lighting and transmitting source for the white-light VLC.
Photographs of (A) VLD on copper plate and (B) VLD + CdSe/ZnS core-shell-QD white-light source.

for temperature stabilization. A thermistor diode (TD) detected the temperature of the TO-can shell, and a thermoelectric cooler (TEC) fixed between the heat sink and the copper plate handled and isolated the heat transfer in one direction. Both the TD and TEC were connected to a temperature controller (Newport Corporation, Irvine, CA, USA, LDC-3900) so that the temperature can be precisely stabilized by automatically adjusting the operating current of the TEC. Then, the heat transferred to the aluminum-fin heat sink was further dissipated via the electric fan. In this way, the homemade self-feedback temperature controller system flexibly adjusted and effectively controlled the VLD at room temperature of 25°C with a small variation of ± 0.05°C.

To demonstrate the VLD based indoor white-lighting application, the CdSe/ZnS core-shell QDs doped PDMS film was employed as the color converter for transferring the violet-blue beam into the divergent white-light spot, which was fabricated by embedding the CdSe/ZnS core-shell QDs with luminescent wavelengths of 515 nm and 630 nm into PDMS aqueous solution, as Figure 2 illustrates. Various solutions mixed with the dual-size QDs by different ratios were prepared for testing to achieve the desirable CCT. As PLQYs of CdSe/ZnS core-shell-QD solutions with different emission wavelengths are slightly different, the amount of red and green CdSe/ZnS core-shell QDs in the PDMS aqueous solution is not exactly equivalent with each other. After measuring several films with different mixing recipes, the optimized CdSe/ZnS core-shell-QD doped PDMS colored light converter is obtained with a mixing density ratio of 1:6. With the chosen ratio, the CdSe/ZnS core-shell-QD mixed solution was further diluted by toluene with a mixing ratio of 1:3, and subsequently diluted by PDMS solution with a mixing ratio of 1:2. To solidify such a compound solution, it was poured into a circle mold and baked at 30°C. After baking for 6 h or longer, the solution was solidified to a yellowish-orange translucent film with a thickness of 2.5 mm and a diameter of 16 mm.

The experimental setup of the CdSe/ZnS core-shell-QD assisted VLD white-lighting communication system is shown in Figure 3A. To measure the transmission performance of the white-lighting VLD + CdSe/ZnS core-shell-QD source with off-line encoding/decoding analysis, an AWG (Tektronix, Beaverton, OR, USA, 70001A) with a sampling rate of 12 GS/s was used to delivered the 16-QAM DMT data with the FFT-size of 512 and a power of –2 dBm [a peak-to-peak amplitude (V_{pp}) of 500 mV]. Note that the 16-QAM DMT data was generated by the pseudo-random bit sequence data with a length of 2^{15}–1. Figure 3B illustrates the block diagram for the algorithm of the 16-QAM DMT data. In the data stream, the cyclic prefix was replaced with a series of the Chebyshev filters with a filter window length of 220 to avert unwanted crosstalk between data delivered by neighboring subcarriers. Afterwards, a microwave amplifier (Tektronix, Beaverton, OR, USA, 5866) with 10-GHz bandwidth and

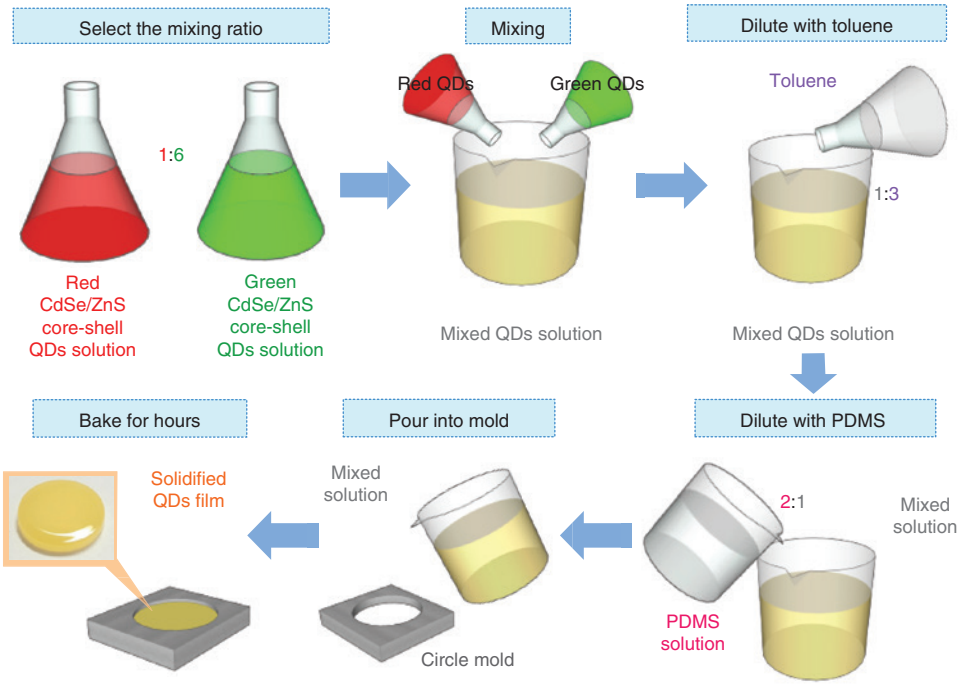

Figure 2: Fabrication method of CdSe/ZnS core-shell-QD doped PDMS film.

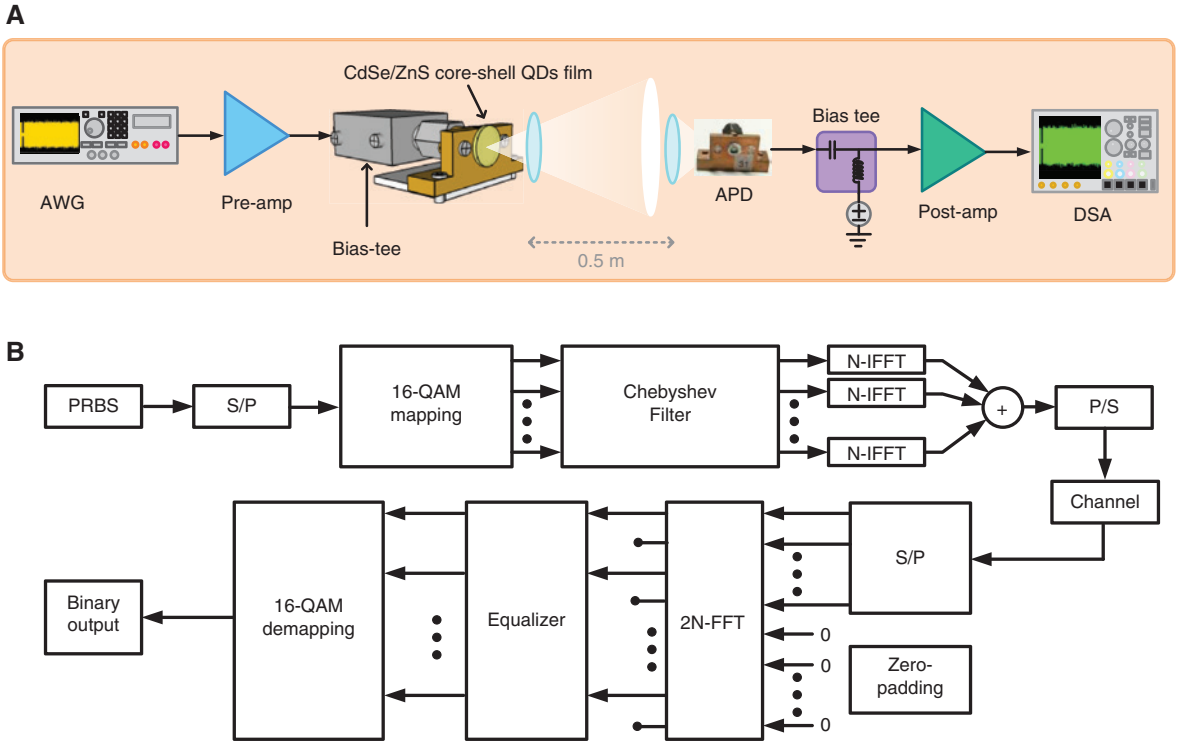

Figure 3: Experimental and modulation scheme of the VLD + CdSe/ZnS core-shell-QD-based white-lighting VLC system. (A) Experimental setup of 0.5-m VLD + CdSe/ZnS core-shell-QD-based white-lighting VLC system. (B) The block diagram for the algorithm of the 16-QAM DMT data.

25-dB gain magnified the power of the 16-QAM DMT data stream to 11 dBm (V_{pp} = 2.2 V), and the data stream was combined with the DC current via a bias-tee (Mini Circuits, Brooklyn, NY, USA, ZX85-12G-S+) for directly modulating the VLD at the optimized biased point. Then, the bias-tee was connected to the VLD packaged with an SMA connector. After adhering the CdSe/ZnS core-shell-QD doped PDMS film based color converter to the output window of the VLD for white-light generation, a plano-convex lens with a focal length of 5 cm and a diameter of 5 cm was placed in front of the VLD to collimate the divergent laser beam, and the collimated beam propagated in free space over a 0.5-m link. At the receiving end, a convex lens with a focal length of 5 cm and a diameter of 5 cm was used to collect part of the optical signal into a 110-V negatively biased avalanche photodiode (APD, AD230-8 TO) with a receiving bandwidth of 2 GHz. For the receiver output, a bias-tee (Tektronix, Beaverton, OR, USA, 55530B) separated the DC bias from the converted AC signal, and the received 16-QAM DMT datastream was further amplified via an amplifier (Mini Circuits, Brooklyn, NY, USA, ZX60-V63+) with a power gain of 20 dB and the 3-dB bandwidth of 6 GHz. Finally, a real-time digital serial analyzer (Tektronix, Beaverton, OR, USA, 71604C) with a resolution of 100 GS/s sampled the waveform of the received signal, and a homemade MATLAB program was employed to decode the data from the waveform after FFT and analog-to-digital converter (ADC) process. The constellation plot, the error vector magnitude (EVM), the signal-to-noise ratio (SNR) and the bit error ratio (BER) were analyzed to evaluate the transmission performance. For the QAM-DMT data, the SNR was calculated using SNR ≈ EVM^{-2}, and the BER can be obtained by calculating the relationship between the EVM and BER, which is expressed as [4, 32–34]:

$$BER \cong \frac{2\left(1-\frac{1}{\sqrt{M}}\right)}{\log_2 M} \times \left\{ \operatorname{erfc}\left[\frac{1}{\mathrm{EVM}}\sqrt{\frac{3}{2(M-1)}}\right] + \operatorname{erfc}\left[\frac{3}{\mathrm{EVM}}\sqrt{\frac{3}{2(M-1)}}\right]\right\}, \quad (1)$$

where M denotes the QAM level. Equation (1) clearly indicates that the BER will be lower than 3.8×10^{-3} if the EVM remains less than 17.39%. On the other hand, the CCT, CRI and Commission International de l'Eclairage (CIE) coordinate of the VLD + CdSe/ZnS core-shell-QD color converted white-light source were analyzed by a colorimeter (OKTEK, New Taipei City, Taiwan, GL-2). Similarly,

an illuminometer (TECPEL, New Taipei City, Taiwan, 530) with an aperture diameter of 1 cm measured the illuminance of the white-light spot to evaluate its maximal brightness and divergent angle.

3 Results and discussion

3.1 Lasing and modulating characteristics of the violet laser diode

Figure 4A shows the power-current-voltage (P-I-V) response of the VLD with a threshold current of 30 mA, which indicates a *dP/dI* slope of 0.69 W/A and a maximal output power of 60 mW. In general, such an output power level should be sufficiently high to provide required illuminance for indoor-lighting purpose. Notwithstanding, the overly high VLD power may result in residual blue light component to cause a hazard to human eyes, which can be balanced with excited fluorescence after color conversion such that the synthesized white-light can provide an acceptable CCT value. Considering the mentioned requirement, the VLD with the maximal output power of 60 mW is selected to match with the CdSe/ZnS core-shell-QD doped PDMS film in this work. The lasing spectrum of the employed VLD revealed in Figure 4B shows a peak emission wavelength at 406 nm with a full width at half-maximum (FWHM) of 3 nm. Before testing the practical transmission performance of the 16-QAM DMT data carried by the VLD, the analog modulation frequency response is measured to preliminarily determine the allowable bandwidth for encoding the 16-QAM DMT data. Accordingly, Figure 4C shows the small-signal modulation frequency response of the VLD operated at different bias currents, indicating the cutoff frequency of 1.16 GHz at −3 dB decay and 1.57 GHz at −6 dB decay when adjusting the VLD bias up to 50 mA. In detail, the relaxation oscillation peak noticeably up-shifts from 2.2 to 3.5 GHz as the bias current of the VLD increases from 30 to 60 mA, providing a flattened response curve without affecting by the relaxation oscillation induced relative intensity noise. Although enlarging the bias current of the VLD somewhat broadens the modulation frequency bandwidth and extends the modulation response to high-frequency region, the roll-off effect significantly declines the power-to-frequency slope so as to reduce the throughput intensity concurrently, which is due to the conversion of low-frequency throughput to high frequencies when up-shifting

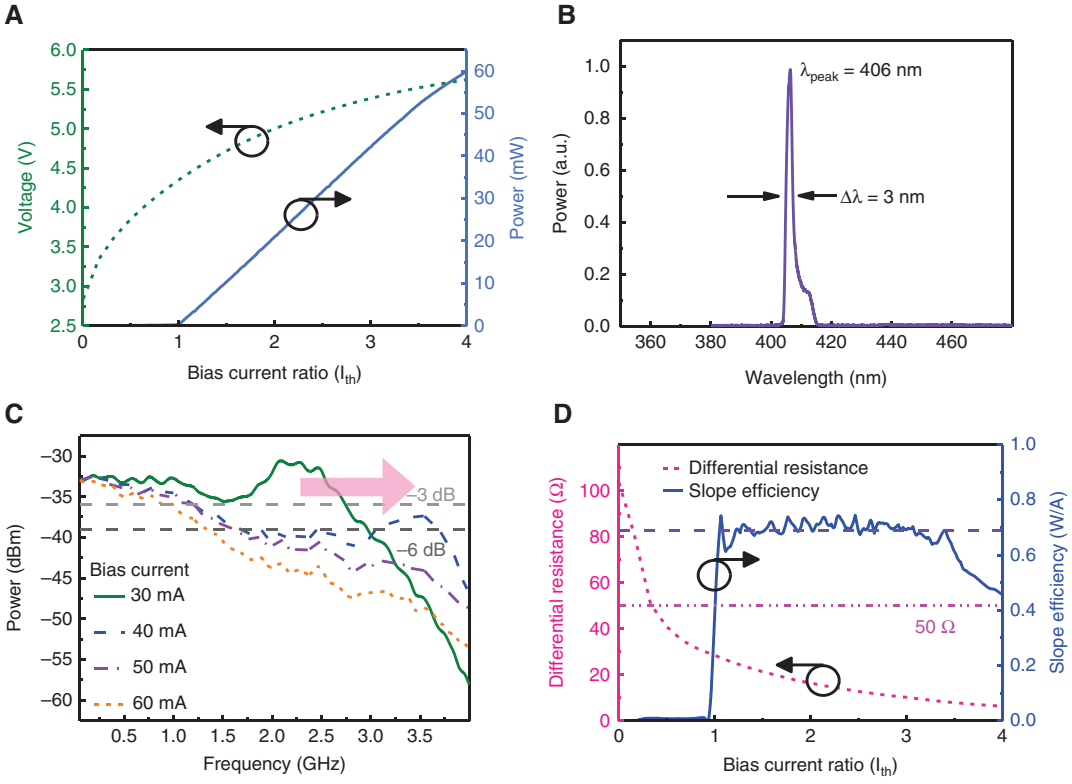

Figure 4: Lasing and modulating characteristics of the VLD.
(A) P-I-V curve, (B) lasing spectrum, (C) frequency response, and (D) differential resistance and slope efficiency of VLD.

relaxation oscillation frequency of the VLD with increasing its bias current [35, 36]. Figure 4D shows the differential resistance (*dV/dI*) and slope efficiency (*dP/dI*) of the VLD, which is, respectively, calculated by differentiating voltage and power with currents. The average slope efficiency beyond threshold is about 0.69 W/A, and the differential resistance at the bias current of 50 mA (~$1.6I_{th}$) is 19.5 Ω, which is smaller to the resistance of the general RF component of 50 Ω. To estimate the impedance mismatch, the corresponding reflection coefficient (Γ) of −0.439 is calculated as $\Gamma=(Z_{LD}-50)/(Z_{LD}+50)$, and the related voltage standing wave ratio (VSWR) of 2.57 is defined as $[VSWR=(1+|\Gamma|)/(1-|\Gamma|)]$, which indicates the return loss $[\eta_{RL}=-20\log_{10}(|\Gamma|)]$ of 7.15 dB.

3.2 The white-lighting performance of the VLD + CdSe/ZnS core-shell-QD source

Figure 5A illustrates the bird's-eye view photograph of the white-lighting source constructed by adhering the CdSe/ZnS core-shell-QD doped PDMS film to the VLD output window. The white-light is generated by mixing the excited red and green fluorescent components with remaining violet laser light under a spectral power ratio of violet:green:red = 4.4:1:1.5. As the VLD power is adjusted to detune the relative power ratio, a white-light source with variable CCT can be produced. Figure 5B reveals the picture of the white-light spot captured on a white-paper, which was collimated by a convex lens located at 50 cm from the VLD + CdSe/ZnS core-shell-QD output. Besides, Figure 5C reveals the angle-dependent illuminance measured at distances of 50 cm and 20 cm from the output, where 0° represents the central axis of the light under collimation. At 20 cm away from the VLD + CdSe/ZnS core-shell-QD output, the illuminance of 11 lux is obtained at 0°. While expanding distance to 50 cm, the illuminance at central axis reduces to 2.75 lux. Even though the illuminance is less than the commercial light source, the drawback could be solved considerably by using the VLD array covered with large-area CdSe/ZnS core-shell-QD doped PDMS film. Moreover, the divergent angle (θ_{-3dB}) of the VLD + CdSe/ZnS core-shell-QD source is 127°, which is defined by the angle at the half maximal illuminance. With the CdSe/ZnS core-shell-QD doped PDMS film, the radiant angle of the laser light is effectively expanded, and the brightness of the white light is uniform.

To further characterize the quality of the proposed VLD + CdSe/ZnS core-shell-QD phosphor mixed white light, the CCTs, the CRIs, and the CIE chromaticity coordinates are measured. Figure 6A reveals CCT and CRI values of the white-light generated by changing the VLD biased from 35 mA to 60 mA. In principle, when the excited fluorescence has reached its saturation condition, further raising the bias current could merely increase the CCT value as the portion of the violet light is linearly increased without converting into colored fluorescence. On the contrary, the CRI of the color converted

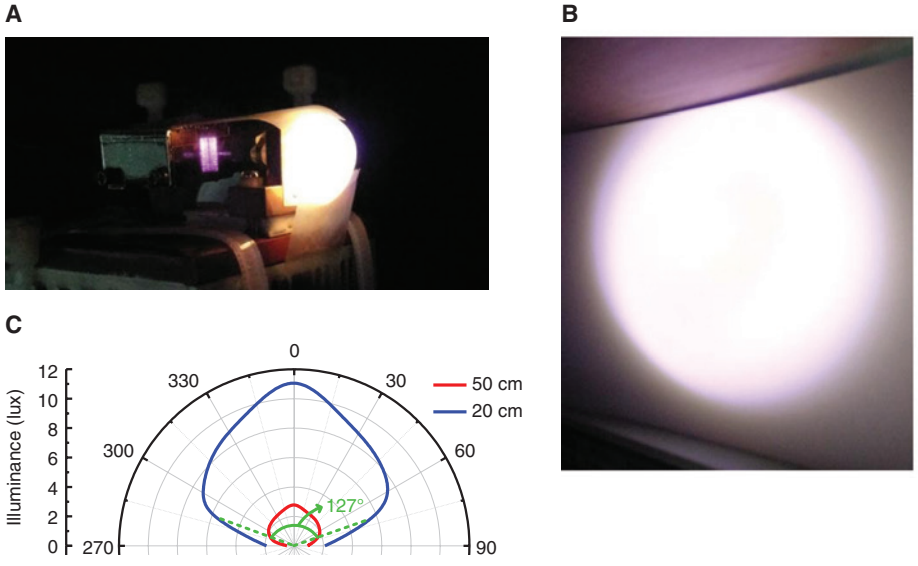

Figure 5: The performance of the white-lighting source constructed by adhering the CdSe/ZnS core-shell-QD doped PDMS film to the VLD output window.
(A) Photograph of VLD + CdSe/ZnS core-shell-QD base white-lighting source; (B) photograph of white-light spot collimated by a convex lens; (C) angle-dependent illuminance distribution of VLD + CdSe/ZnS core-shell-QD base white-lighting source.

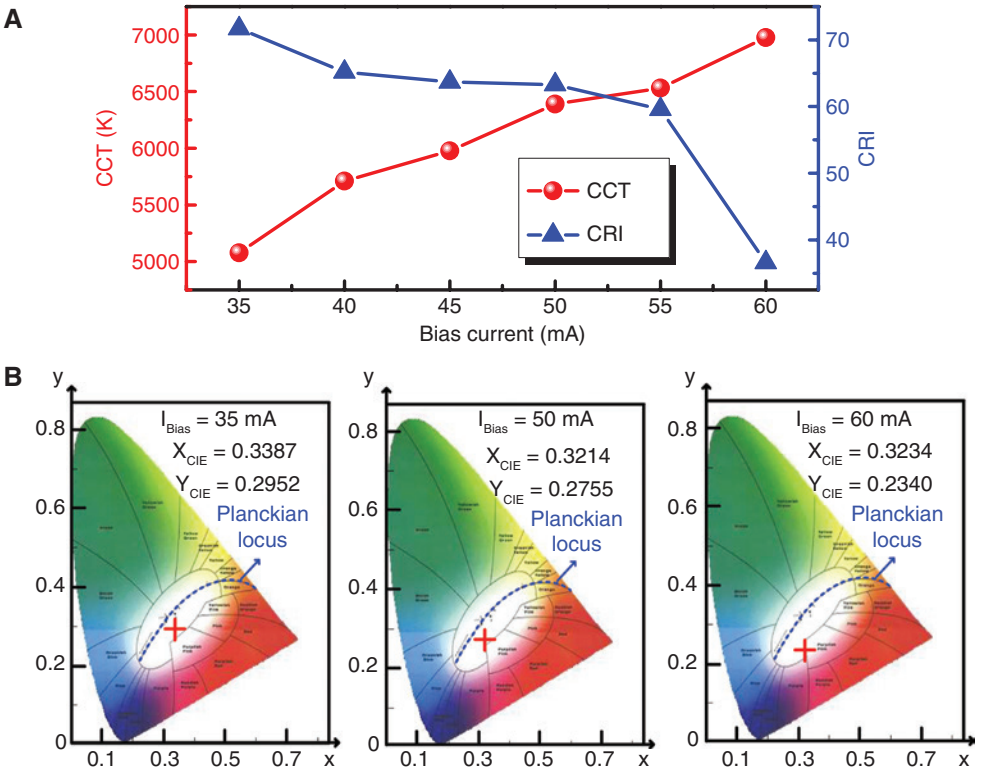

Figure 6: The quality of the VLD + CdSe/ZnS core-shell-QD phosphor mixed white light.
(A) CCTs and CRIs of VLD + CdSe/ZnS core-shell-QD based white-lighting source at different bias currents; (B) CIE coordinates of VLD + CdSe/ZnS core-shell-QDs based white-lighting source biased at 35, 50, and 60 mA.

white-light seems to be decreased as the bias current of the VLD reduces due to the excessive violet light component. Figure 6B shows the CIE coordinate of the VLD + CdSe/ZnS core-shell-QD based light source at different bias currents on the CIE 1931 chromaticity diagram with a Planckian locus curve. When biasing at 35 mA, the synthesized white-light exhibits a CCT of 5078 K, a CRI of 71.7 and, a CIE coordinate at 0.3387, 0.2952. With operating the VLD at bias current of 50 mA, the optimized cold white-lighting case appears with a CCT of 6389 K, a CRI of 63.3 and a CIE coordinate at 0.3214, 0.2755. By continuously increasing the bias current to 55 mA, the CRI further reduces to 59.6 even though a CCT of 6531 K with a CIE coordinate at 0.3224, 0.2577 can be achieved. The CCT keeps enlarged from nearly 6500 K to 6976 K with the CIE coordinate at 0.3234, 0.2340 when enlarging the VLD bias to 60 mA, whereas the CRI seriously decreases to 36.6, which cannot meet the demanded lighting requirement. Increasing the bias current can effectively enhance the VLD power, which indicates that the violet component in mixed white light also increases to degrade the CRI of mixed white light. As a result, setting the bias current at 50 ~ 55 mA is the considerably desired working point for both indoor lighting and white-lighting communication purposes. In this work, the CdSe/ZnS core-shell QDs only contribute to the green and red color components for mixing white light. As compared to previous work [37], the mixed white-light in this work with decreased CRI is due to the lack of yellow-orange color component. Therefore, the CRI of this mixed white light can be improved by the aid of the fourth colored light.

Although adhering the CdSe/ZnS core-shell-QD doped PDMS film on to the VLD output window can provide not only the yellow-light conversion but also the divergent angle enlargement for lighting purpose, the transmission performance would be sacrificed to a certain degree inevitably. As the most part of the violet light interacts with the CdSe/ZnS core-shell QDs for the color conversion, the residual power of the violet light penetrated through the CdSe/ZnS core-shell-QD doped PDMS has attenuated accordingly. Figure 7A plots the power-to-current responses before and after adhering the CdSe/ZnS core-shell-QD doped PDMS film on to the VLD window. Note that the wavelength of the employed power meter is set at 405 nm so as to exclude the power of excited yellow fluorescence. In detail, the power-to-current slope efficiency decreases from 0.69 to 0.21 W/A, indicating the severely degraded power of violet light with color conversion and scattering process. Additionally, Figure 7B shows the analog modulation frequency response of the VLD + CdSe/

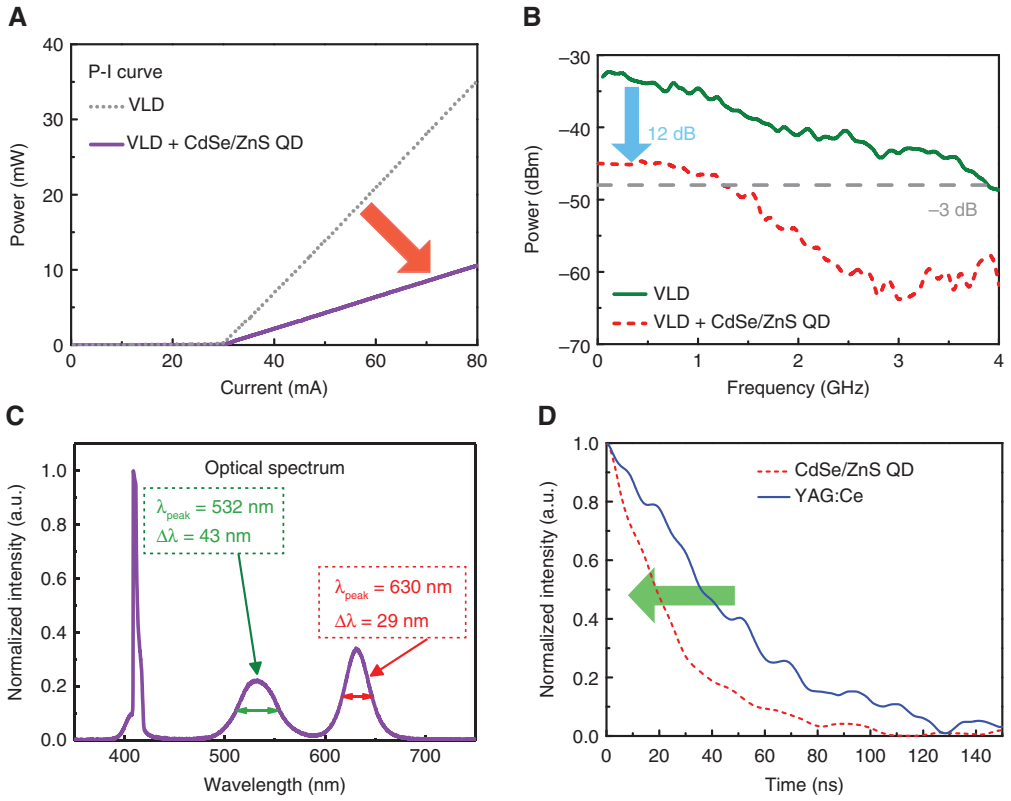

Figure 7: The modulation characteristic of the VLD before and after adhering CdSe/ZnS core-shell-QD doped PDMS film. (A) Power-to-current curve before and after adhering CdSe/ZnS core-shell-QD doped PDMS film; (B) frequency response and (C) optical spectrum of VLD + CdSe/ZnS core-shell-QD based white-lighting source; (D) TRPL response of CdSe/ZnS core-shell QDs.

ZnS core-shell-QD based white-lighting source at the bias current of 50 mA. As compared to the modulation frequency response of the VLD biased at 50 mA without adhering the CdSe/ZnS core-shell-QD doped PDMS film (Figure 7B), the frequency response of the VLD + CdSe/ZnS core-shell-QD white-lighting source exhibits an overall throughput power degradation of 12 dB with its slope noticeably declined at higher than 2 GHz. It is mainly caused by the scattering and absorption in the CdSe/ZnS core-shell-QD doped PDMS film, and the slow photoluminescent lifetime of the CdSe/ZnS core-shell QDs may slightly deteriorate the frequency response. Furthermore, Figure 7C shows the color-converted optical spectrum of the VLD + CdSe/ZnS core-shell-QD in which the red and green fluorescent components with peak wavelengths of 630 and 532 nm are observed, respectively. Unlike the traditional phosphor material, the CdSe/ZnS core-shell-QD doped PDMS film can provide a wideband fluorescence, the red/green fluorescence with a relatively narrow FWHM of 29/43 nm is mainly contributed by the CdSe/ZnS core-shell-QDs of the different size due to quantum confinement effect. Subsequently, the time-resolve photoluminescence (TRPL) analysis is performed to estimate the photon lifetime of the CdSe/ZnS core-shell QDs, as shown in Figure 7D. For comparison, the TRPL response of the YAG:Ce^{3+} powder that is commonly used for white-light LEDs, is also demonstrated. Apparently, the mixed CdSe/ZnS core-shell QDs reveals a photon lifetime of 23.8 ns, which is much shorter than that of 52.7 ns for the YAG:Ce^{3+} phosphor. This analysis confirms the shorted TRPL lifetime of the CdSe/ZnS core-shell-QD based spontaneous emission that can be obtained after color-converting the VLD output.

3.3 The white-lighting transmission performance of the VLD + CdSe/ZnS core-shell-QD

For indoor free-space white-lighting communication, the transmission performance of the VLD + CdSe/ZnS core-shell-QD white-lighting system is analyzed. Particularly, different AWG sampling rates for the QAM-DMT data and bias currents for the VLD are respectively optimized to reach the ultimate transmission bandwidth. Figure 8A shows the received BERs of the original 2.1-GHz 16-QAM DMT data generated by the AWG with different sampling rates, and their complementary cumulative distribution

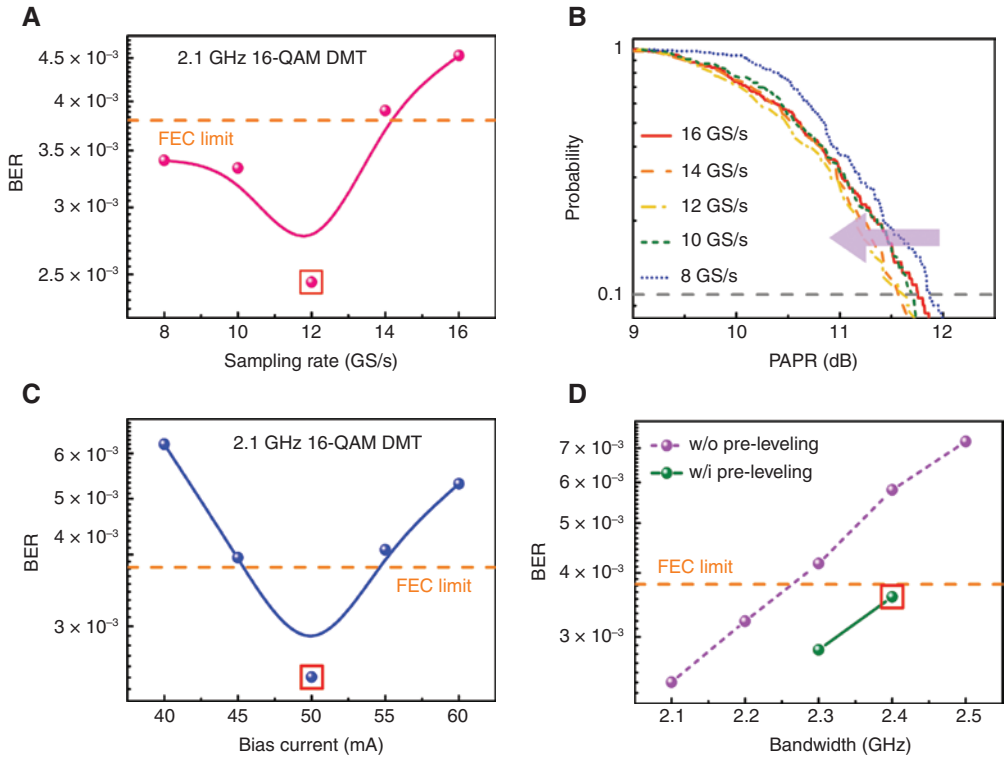

Figure 8: The white-lighting transmission performance of the VLD + dSe/ZnS core-shell-QD at different operating conditions. (A) BERs and (B) PAPRs of 2.1-GHz 16-QAM DMT data transmitted by the VLD adhered with the CdSe/ZnS core-shell-QD doped PDMS film at different sampling rates; (C) BERs of 2.1-GHz 16-QAM DMT data at different bias currents; (D) BERs of 16-QAM DMT data at different bandwidths before and after pre-leveling.

function (CCDF) curves of the measured peak-to-average power ratio (PAPR) are compared in Figure 8B. By increasing the sampling rate from 8 to 12 GS/s, the 16-QAM DMT data stream decreases its subcarrier number (subcarrier number = FFT size × bandwidth/sampling rate) from 135 to 90 and increases its upsampling factor (upsampling factor = sampling rate/bandwidth) from 3.81 to 5.71, respectively, which could scale down the probability for generating the high-peak-amplitude waveform in time domain. Hence, the PAPR at the probability of 10^{-1} slightly decreases from 11.9 to 11.6 dB, and the received BER can be optimized from 3.4×10^{-3} to 2.5×10^{-3} by increasing the sampling rate from 8 to 12 GS/s. Notwithstanding, when the sampling rate is set at 16 GS/s, the PAPR at the probability of 10^{-1} increases to 11.8 dB, which causes a degraded BER of 4.5×10^{-3}. Hence, the AWG sampling rate is set as 12 GS/s for the VLD carried 16-QAM DMT data to obtain the optimal data bandwidth. Similarly, the bias current of the VLD is optimized for improving the BER of the received 2.1-GHz 16-QAM DMT data stream with a sampling rate of 12 GS/s, as shown in Figure 8C. To improve the SNR when modulating the VLD, the AWG outputs the electrical 16-QAM DMT data with the maximum V_{pp} of 500 mV. To optimize the SNR, the V_{pp} needs to be boosted up to 2.2 V at the transmitted end by a microwave amplifier with 10-GHz bandwidth and 25-dB gain. After receiving, the Vpp become 170 mV by post-amplifying with an amplifier with 6-GHz bandwidth and a 20-dB gain. When adjusting the VLD bias from 40 to 50 mA, the received BER improves from 6.2×10^{-3} to 2.5×10^{-3} with the reduced waveform clipping, enlarged throughput intensity, improved SNR, and restrained relative intensity noise (RIN). Nevertheless, continuously raising the bias current to 60 mA would conversely degrade the received BER to 5.3×10^{-3}, declaring that the bias current of 50 mA is the optimized bias current for the white-lighting communication. When employing the VLD as the VLC transmitter, properly raising the bias current can suppress the impact of waveform clipping, frequency chirp, and RIN on the carried 16-QAM DMT data. Even though such an operation is usually accompanied with the drawback of the declined frequency response [38], a trade-off between the bias current and frequency response declination is set for carrying the 16-QAM DMT data. Subsequently, the data bandwidth is further extended under the optimized operating condition. Figure 8D shows the received BER versus different bandwidth with and without implementing the DMT subcarrier amplitude pre-leveling. Pre-leveling is a digital

signal processing technology to facilitate the allowable QAM-DMT data bandwidth when directly modulating the VLD, which redefines each DMT subcarrier powers with a positive slope to overcome the declined frequency response of the VLD [39]. Such a technology strengthens the attenuated DMT subcarrier powers at high frequencies by slightly sacrificing the DMT subcarrier powers at low frequencies so as to improve the average SNR of the whole DMT data stream. Without pre-leveling, the maximal bandwidth can only reach 2.2 GHz with an EVM of 17.02%, an SNR of 15.38 dB and a BER of 3.22×10^{-3}. After pre-leveling, the modulation bandwidth can be further enlarged to 2.4 GHz with optimizing the upsampling factor to 5.

At the data bandwidth of 2.4 GHz, the received BERs of 16-QAM DMT data can be improved by applying different pre-leveling slopes, as shown in Figure 9A. When setting the pre-leveling slope as 0.1 dB/GHz, the received BER of 4.8×10^{-3} indicates that the delivered optical power at high-frequency region is not appropriately enhanced. By increasing the pre-leveling slope to 0.3 dB/GHz, an FEC criterion qualified BER of 3.6×10^{-3} is acquired. Further enlarging the pre-leveling slope to larger than 0.4 dB/GHz severely sacrifices the power of data carried by low-frequency subcarriers, which degrades its related BER beyond 5.4×10^{-3}. After transmitting the pre-leveled 2.4-GHz 16-QAM DMT data delivered by the VLD + CdSe/ZnS core-shell-QD based white-light source, Figure 9B plots the SNRs of the data carried by different subcarrier with the corresponding EVM of 17.26%, SNR of 15.26 dB and BER of 3.6×10^{-3}. Moreover, the fast Fourier transformed RF spectrum shown in Figure 9C exhibits a carrier-to-noise ratio (CNR) of 11 dB, and Figure 9D reveals a clear constellation plot of the received 2.4-GHz 16-QAM DMT data.

In previous work, Xiao et al. used the blue LED combining with CdSe/ZnS core-sell QD to perform the white-lighting visible light communication [31]. However, the 3-dB modulation bandwidth of the blue LED and CdSe/ZnS core-sell QD mixed white light is only 2.6 MHz. In this work, the VLD can effectively enhance its modulation bandwidth to 1.25 GHz after mixing white lighting for improving its transmission performance. In addition, replacing the light source to the VLD can effectively decrease the eye hazard to protect the human eye as compared to blue LD or LED because the spectral weighing value at 405 nm for blue-light hazard function is 6 times lower than that at 450 nm [40]. Therefore, this VLD and CdSe/ZnS core-shell

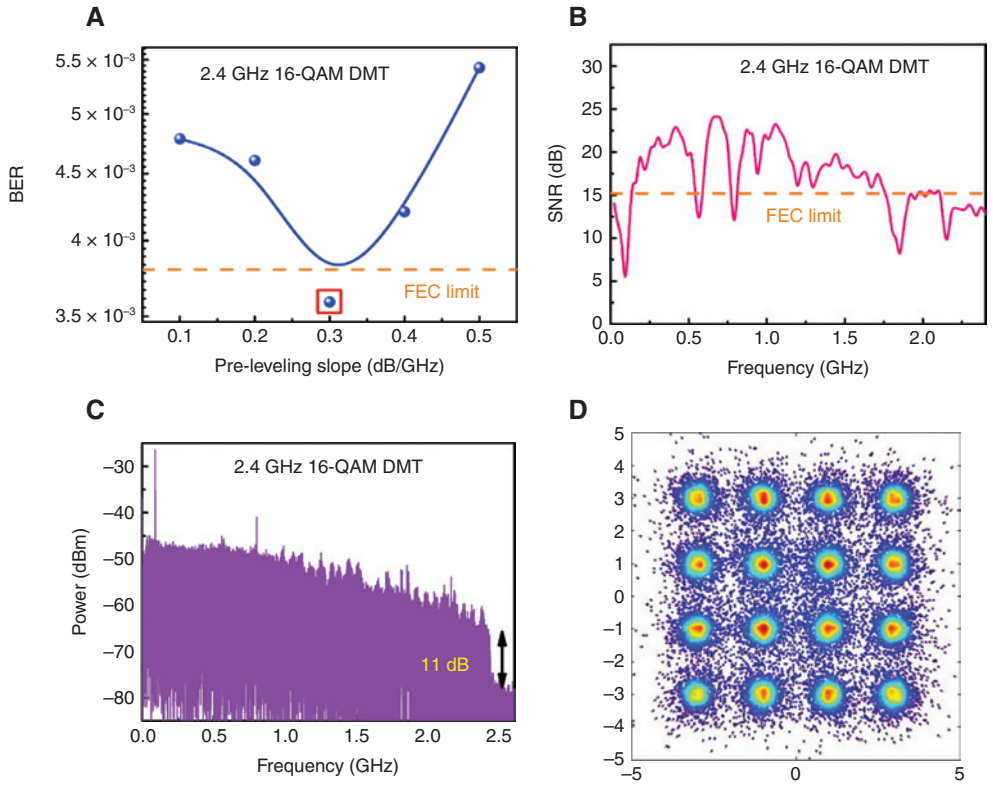

Figure 9: The performance improvement of the 16-QAM DMT data carried by the VLD + CdSe/ZnS core-shell-QD based white-lighting source with the pre-leveling.
(A) BERs of 2.4-GHz 16-QAM DMT data transmitted by VLD + CdSe/ZnS core-shell-QD based white-lighting source at different pre-leveling slopes. (B) Subcarrier SNRs, (C) RF spectrum, and (D) constellation plot of 2.4-GHz 16-QAM DMT data at optimized pre-leveling slope.

QDs mixed white-light not only improves the transmission performance but also suppresses the eye hazard. In our case, the bias current of the VLD is set as small as 50 mA ($1.6I_{th}$) to obtain the optimized QAM-OFDM transmission performance with a data rate of 9.6 Gbit/s and a BER of 3.59×10^{-3}. Owing to such low bias, this VLD also performs extremely low lighting illuminance after color conversion with CdSe/ZnS core-shell QD phosphor. As the responsivity of the commercial illuminometer at 405 nm is only 0.0008 (much lower than that of 0.038 at 450 nm [41]), the output power of 12.4 mW for VLD biased at 50 mA can hardly provide sufficient illuminance for indoor lighting. On the other hand, the phosphor plate with low volume density of CdSe/ZnS core-shell QDs also provides a low color conversion efficiency to result in low illuminance. Therefore, the illuminance of the VLD + CdSe/ZnS mixed white light is only 11 lux. In future work, it is mandatory to increase both the VLD power (using VLD array) and the QD density to effectively enhance the illuminance for indoor lighting.

4 Conclusion

With using the dual-size CdSe/ZnS core-shell-QD doped PDMS film as the phosphor color converter to enhance the CRI, the VLLC system with high HSV and CRI based on the VLD + CdSe/ZnS core-shell-QD source for both indoor white-lighting and high-speed communication is successfully demonstrated. The VLD + CdSe/ZnS core-shell-QD white-light source by sacrificing part of the violet light for necessary color conversion exhibits a CCT of 6389 K, a CRI of 63.3 and a CIE coordinate at 0.3214, 0.2755 with a divergent angle of 127°, which is qualified for the ordinary indoor lighting purpose. By optimizing the operation conditions of the VLD and the sampling rate of the AWG, the delivered 16-QAM DMT data stream reaches a modulation bandwidth as wide as 2.2 GHz with an EVM of 17.0%, an SNR of 15.4 dB and a BER of 3.2×10^{-3}. With pre-leveling, the DMT subcarrier at an optimized slope of 0.3 dB/GHz compensates the insufficient SNR of the high-frequency subcarrier delivered data so that the VLD + CdSe/ZnS core-shell-QD based white-light source can carry 16-QAM DMT data at 9.6 Gbit/s with an EVM of 17.3%, SNR of 15.3 dB, and an FEC-demanded BER of 3.6×10^{-3}. This work proves the capability of the CdSe/ZnS core-shell-QD for efficiently color-converting the VLD to the white light with fast radiative recombination in CdSe/ZnS core-shell QDs, which not only shortens the luminescent lifetime but also adjusts the CCT to provide efficient lighting with warm-white, cool-white and daylight colors for different circumstances. By adding dual-size CdSe/ZnS core-shell QDs to provide versatile luminescent bands, it is expectable that the CRI can be further enhanced to fulfill the demand of the high-quality white-lighting application.

Acknowledgment: The work was supported by the Ministry of Science and Technology, Taiwan, R.O.C., under grants MOST 106-2221-E-002-152-MY3, MOST 107-2221-E-002-159-MY3, MOST 107-2221-E-002-158-MY3, and MOST 107-2218-E-992-304-, Funder Id: http://dx.doi.org/10.13039/501100004663.

References

[1] Minh HL, O'Brien D, Faulkner G, et al. High-speed visible light communications using multiple-resonant equalization. IEEE Photon Technol Lett 2008;20:1243–5.
[2] Vucic J, Kottke C, Nerreter S, Langer K-D, Walewski JW. 513 Mbit/s visible light communications link based on DMT-modulation of a white LED. J Lightw Technol 2010;20:3512–8.
[3] Khalid AM, Cossu G, Corsini R, Choudhury P, Ciaramella E. 1-Gb/s transmission over a phosphorescent white LED by using rate-adaptive discrete multitone modulation. IEEE Photon J 2012;20:1465–73.
[4] Cossu G, Khalid AM, Choudhury P, Corsini R, Ciaramella E. 3.4 Gbit/s visible optical wireless transmission based on RGB LED. Opt Exp 2012;24:B501–6.
[5] Wu FM, Lin CT, Wei CC, et al. Performance comparison of OFDM signal and CAP signal over high capacity RGB-LED-based WDM visible light communication. IEEE Photon J 2013;5:7901507.
[6] Wang Y, Wang Y, Chi N, Yu J, Shang H. Demonstration of 575-Mb/s downlink and 225-Mb/s uplink bi-directional SCM-WDM visible light communication using RGB LED and phosphor-based LED. Opt Exp 2013;21:1203–8.
[7] Wang Y, Huang X, Tao L, Shi J, Chi N. 4.5-Gb/s RGB-LED based WDM visible light communication system employing CAP modulation and RLS based adaptive equalization. Opt Exp 2015;23:13626–33.
[8] Huang X, Chen S, Wang Z, et al. 2.0-Gb/s visible light link based on adaptive bit allocation OFDM of a single phosphorescent white LED. IEEE Photon J 2015;7:7904008.
[9] Philips steps up its commitment to Li-Fi, with trial in Paris. LEDs Magazine. Nashua, New Hampshire, USA. Available at: http://www.ledsmagazine.com/articles/2018/03/philips-steps-up-its-commitment-to-li-fi-with-trial-in-paris.html. Accessed: 16 Mar 2018.
[10] Li X, Bamiedakis N, Guo X, et al. Wireless visible light communications employing feed-forward pre-equalization and PAM-4 modulation. J Lightw Technol 2016;34:2049–55.
[11] Ferreira RXG, Xie E, McKendry JJD, et al. High bandwidth GaN-based micro-LEDs for multi-Gb/s visible light communications. IEEE Photon Technol Lett 2008;20:1243–5.
[12] Islim MS, Ferreira RX, He X, et al. Towards 10 Gb/s orthogonal frequency division multiplexing-based visible light communication sing a GaN violet micro-LED. Photon Res 2017;5:A35–43.

[13] Chi Y-C, Hsieh D-H, Tsai C-T, Chen H-Y, Kuo H-C, Lin G-R. 450-nm GaN laser diode enables high-speed visible light communication with 9-Gbps QAM-OFDM. Opt Exp 2015;23:13051–9.
[14] Lee C, Shen C, Oubei HM, et al. 2 Gbit/s data transmission from an unfiltered laser-based phosphor-converted white lighting communication system. Opt Exp 2015;23:29779–87.
[15] Retamal JRD, Oubei HM, Janjua B, et al. 4-Gbit/s visible light communication link based on 16-QAM OFDM transmission over remote phosphor-film converted white light by using blue laser diode. Opt Exp 2015;23:33656–66.
[16] Chi Y-C, Hsieh D-H, Lin C-Y, et al. Phosphorous diffuser diverged blue laser diode for indoor lighting and communication. Sci Rep 2015;5:18690.
[17] Chun H, Rajbhandari S, Tsonev D, Faulkner G, Haas H, O'Brien D. Visible light communication using laser diode based remote phosphor technique. In: Proceedings of IEEE International Conference on Communications Workshop. London, UK, IEEE, 2015, pp. 1392–7.
[18] Wu T-C, Chi Y-C, Wang H-Y, et al. White-lighting communication with a Lu3Al5O12:Ce3+/CaAlSiN3:Eu2+ glass covered 450-nm InGaN laser diode. J Lightw Technol 2018;36:1634–43.
[19] Tsonev D, Videv S, Haas H. Towards a 100Gbps visible light wireless access network. Opt Exp 2015;23:1627–37.
[20] Janjua B, Oubei HM, Retamal JRD. Going beyond 4 Gbps data rate by employing RGB laser diodes for visible light communication. Opt Exp 2015;23:18746–53.
[21] Wu T-C, Chi Y-C, Wang H-Y, Tsai C-T, Huang Y-F, Lin G-R. Tricolor R/G/B laser diode based eye-safe white lighting communication beyond 8 Gbit/s. Sci Rep 2017;7:11.
[22] Chi Y-C, Huang Y-F, Wu T-C, et al. Violet laser diode enables lighting communication. Sci Rep 2017;7:10469.
[23] Lee C, Shen C, Cozzan C, et al. Gigabit-per-second white light-based visible light communication using near-ultraviolet laser diode and red-, green-, and blue-emitting phosphors. Opt Exp 2017;25:17480–7.
[24] Chun H, Manousiadis P, Rajbhandari S, et al. Visible light communication using a blue GaN μLED and fluorescent polymer colour converter. IEEE Photon Technol Lett 2014;26:2035–8.
[25] Sajjad MT, Manousiadis PP, Orofino C, et al. Fluorescent red-emitting BODIPY oligofluorene star-shaped molecules as a color converter material for visible light communications. Adv Opt Mater 2015;3:536–40.
[26] Sajjad MT, Manousiadis PP, Chun H, et al. Novel fast color-converter for visible light communication using a blend of conjugated polymers. ACS Photon 2015;2:194–9.
[27] Dursun I, Shen C, Parida MR, et al. Perovskite nanocrystals as a color converter for visible light. ACS Photon 2016;3:1150–6.
[28] Wang Z, Wang Z, Lin B, et al. Warm-white-light-emitting diode based on a dye-loaded metal-organic framework for fast white-light communication. ACS Appl Mater Interfaces 2017;9:35253–9.
[29] Leitao MF, Santos JMM, Guilhabert B, et al. Gb/s visible light communications with colloidal quantum dot color converters. IEEE J Sel Top Quantum Electron 2017;23:1900810.
[30] Yang X, Shi M, Yu Y, et al. Enhancing communication bandwidths of organic color converters using nanopatterned hyperbolic metamaterials. J Lightw Technol 2018;36:1862–7.
[31] Xiao X, Tang H, Zhang T, et al. Improving the modulation bandwidth of LED by CdSe/ZnS quantum dots for visible light communication. Opt Exp 2016;24:21577–86.
[32] Shafik RA, Rahman MS, Islam AHMR. On the extended relationships among EVM, BER and SNR as performance metrics. Proc ICECE 2006:408–11.
[33] Schmogrow R, Nebendahl B, Winter M, et al. Error vector magnitude as a performance measure for advanced modulation formats. IEEE Photon Technol Lett 2012;24:61–3.
[34] Hillerkuss D. Single-laser 32.5 Tbit/s Nyquist WDM transmission. J Opt Commun Netw 2012;4:715–23.
[35] Lau EK, Zhao X, Sung HK, Parekh D, Chang-Hasnain C, Wu MC. Strong optical injection-locked semiconductor lasers demonstrating >100-GHz resonance frequencies and 80-GHz intrinsic bandwidths. Opt Exp 2008;16:6609–18.
[36] Lau EK, Wong LJ, Wu MC. Enhanced modulation characteristics of optical injection-locked lasers: a tutorial. IEEE J Sel Topics Quantum Electron 2009;15:618–33.
[37] Huang Y-F, Chi Y-C, Cheng C-H, et al. LuAG:Ce/CASN:Eu phosphor enhanced high-CRI R/G/B LD lighting fidelity. J Mater Chem C 2019;7:9556–63.
[38] Tsai C-T, Cheng M-C, Chi Y-C, Lin G-R. A novel colorless FPLD packaged with TO-can for 30-Gbit/s preamplified 64-QAM-OFDM transmission. IEEE J Sel Top Quantum Electron 2015;21:1500313.
[39] Tsai C-T, Chi Y-C, Lin G-R. Power fading mitigation of 40-Gbit/s 256-QAM OFDM carried by colorless laser diode under injection-locking. Opt Exp 2015;23:29065–78.
[40] Price RB, Labrie D, Bruzell EM, Sliney DH, Strassler HE. The dental curing light: a potential health risk. J Occup Environ Hyg 2016;13:639–46.
[41] Database of the illuminometer (TECPEL, 530). Available from: http://www.tecpel.net/files/DLM530_manual_E.pdf.